

# Online Research @ Cardiff

This is an Open Access document downloaded from ORCA, Cardiff University's institutional repository: <https://orca.cardiff.ac.uk/id/eprint/145826/>

This is the author's version of a work that was submitted to / accepted for publication.

Citation for final published version:

Jang, Hyeon-Sik, Kim, Tae-Hoon, Kim, Byeong Geun, Hou, Bo ORCID: <https://orcid.org/0000-0001-9918-8223>, Lee, In-Hwan, Jung, Su-Ho, Lee, Jae-Hyun, Cha, SeungNam, Yang, Cheol-Woong, Kim, Byung-Sung and Whang, Dongmok 2021. Self-catalytic growth of elementary semiconductor nanowires with controlled morphology and crystallographic orientation. *Nano Letters* 21 (23) , pp. 9909-9915. 10.1021/acs.nanolett.1c02982 file

Publishers page: <http://dx.doi.org/10.1021/acs.nanolett.1c02982>  
<<http://dx.doi.org/10.1021/acs.nanolett.1c02982>>

Please note:

Changes made as a result of publishing processes such as copy-editing, formatting and page numbers may not be reflected in this version. For the definitive version of this publication, please refer to the published source. You are advised to consult the publisher's version if you wish to cite this paper.

This version is being made available in accordance with publisher policies.

See

<http://orca.cf.ac.uk/policies.html> for usage policies. Copyright and moral rights for publications made available in ORCA are retained by the copyright holders.



6  
8  
9  
10  
11  
12  
13  
14  
15  
16  
17  
18  
19  
20  
21  
22  
23  
24  
25  
26  
27  
28  
29  
30  
31  
32  
33  
34  
35  
36  
37  
38  
39  
40  
41  
42  
43  
44  
45  
46  
47  
48  
49  
50  
51  
52  
53  
54  
55  
56  
57  
58  
59

# Self-catalytic growth of Elementary Semiconductor Nanowires with Controlled Morphology and Crystallographic Orientation

*Hyeon-Sik Jang<sup>1</sup>, Tae-Hoon Kim<sup>1,2</sup>, Byeong Geun Kim<sup>3</sup>, Bo Hou<sup>4</sup>, In-Hwan Lee<sup>1</sup>, Su-Ho Jung<sup>1</sup>,  
Jae-Hyun Lee<sup>5</sup>, SeungNam Cha<sup>6</sup>, Cheol-Woong Yang<sup>1</sup>, Byung-Sung Kim<sup>1,7\*</sup> and Dongmok  
Whang<sup>1\*</sup>*

<sup>1</sup>School of Advanced Materials Science and Engineering and SKKU Advanced Institute of  
Nanotechnology, Sungkyunkwan University, Suwon 16419, Korea

<sup>2</sup>Department of Materials Science and Engineering, Chonnam National University, Gwangju  
61186, Republic of Korea

<sup>3</sup>Research Development Division Materials and Components Research Team, Gyeongbuk  
Institute of IT Convergence Industry Technology, Kyungsan 38463, Korea

<sup>4</sup>Department of Physics and Astronomy, Cardiff University, Cardiff CF24 3AA, United Kingdom

<sup>5</sup>Department of Energy Systems Research and Department of Materials Science and Engineering,  
Ajou University, Suwon 16499, Korea

<sup>6</sup>Department of Physics, Sungkyunkwan University, Suwon 16419, Korea

<sup>7</sup>Department of Engineering Science, University of Oxford, Parks Road, Oxford OX1 3PJ, UK

1  
2  
3 **Abstract:** While the orientation-dependent properties of semiconductor nanowires have been  
4  
5  
6 theoretically predicted, their study has long been overlooked in many fields owing to the limits to  
7  
8 control the crystallographic growth direction of nanowires (NWs). We present here the orientation-  
9  
10 controlled growth of single-crystalline germanium (Ge) NWs using a self-catalytic low-pressure  
11  
12 chemical vapor deposition process. By adjusting the growth temperature, the orientation of growth  
13  
14 direction in GeNWs was selectively controlled to the  $\langle 110 \rangle$ ,  $\langle 112 \rangle$ , or  $\langle 111 \rangle$  directions on the  
15  
16 same substrate. The NWs with different growth directions exhibit distinct morphological features,  
17  
18 allowing control of the NW morphology from uniform NWs to nanoribbon structures.  
19  
20  
21 Significantly, the VLS-based self-catalytic growth of the  $\langle 111 \rangle$  oriented GeNW suggests that NW  
22  
23 growth is possible for single elementary materials even without an appropriate external catalyst.  
24  
25 Furthermore, these findings could provide opportunities to investigate the orientation-dependent  
26  
27  
28 properties of semiconductor NWs.  
29  
30

31 **Keywords:** chemical vapor deposition, germanium, nanowire, orientation control, self-catalytic  
32  
33  
34  
35 growth.  
36  
37  
38  
39  
40  
41  
42  
43  
44  
45  
46  
47  
48  
49  
50  
51  
52  
53  
54  
55  
56  
57  
58  
60

1  
2  
3 Semiconductor NWs are promising building blocks for nanoscale electronic and optoelectronic  
4  
5 applications due to their unique one-dimensional structure, quantum confinement effects, and  
6  
7 compatibility with existing semiconductor technologies.<sup>1-4</sup> Over the past two decades, varieties of  
8  
9 semiconductor NWs have been realized through well-developed growth techniques which allow  
10  
11 control of the structures, morphologies, and compositions.<sup>5-10</sup> However, the crystallographic  
12  
13 control over the growth orientations of semiconductor NWs remains a significant challenge.  
14  
15 Numerous theoretical and experimental studies have suggested that the properties of NW are  
16  
17 strongly dependent on its crystallographic direction. For example, theoretically, the specific crystal  
18  
19 orientations might induce a unique electronic structure with an indirect-to-direct energy gap  
20  
21 transition and enhanced carrier mobility under strong quantum confinement effects.<sup>11-14</sup>  
22  
23 Experimental studies have also revealed that the crystal orientations of semiconductor NWs have  
24  
25 a significant role in determining the different mechanical, piezoelectric, and photovoltaic  
26  
27 properties of NW-based electronic and energy-harvesting devices.<sup>15-18</sup> These studies related to  
28  
29 orientation-dependent properties of NWs have provoked investigations for control of NW  
30  
31 orientation via metal catalyst engineering, templated synthesis, or metal-assisted chemical  
32  
33 etching.<sup>19-24</sup> In particular, the preferred growth direction of the NWs grown by vapor-liquid-solid  
34  
35 (VLS) growth and oxide-assisted growth (OAG) have been intensively studied. In group-IV  
36  
37 elementary semiconductors, such as Si and Ge, single-crystalline NWs grown by VLS approach  
38  
39 using metal catalyst predominantly grow along the  $\langle 111 \rangle$  direction.<sup>25-26</sup> In contrast,  $\langle 112 \rangle$  or  
40  
41  $\langle 110 \rangle$  directions are energetically favored for NWs grown using the OAG process.<sup>27-28</sup> In our  
42  
43 previous study, a self-catalytic growth method was suggested to synthesize single-crystalline  
44  
45 silicon (Si) and germanium (Ge) NWs.<sup>29</sup> Control over the diameter and in-situ doping of the  
46  
47 semiconductor NWs also demonstrated that this method is well suited for electronic device  
48  
49  
50  
51  
52  
53  
54  
55  
56  
57  
58  
59  
60

1  
2  
3 applications. Here, we demonstrate that the orientation of the self-catalytic GeNWs can be  
4  
5 controlled with the  $\langle 110 \rangle$ ,  $\langle 112 \rangle$ , and  $\langle 111 \rangle$  growth directions. Through a detailed analysis of  
6  
7 the NW growth phenomena, the growth mechanism and the crystal orientation dependence of the  
8  
9 GeNWs were investigated. In particular, in-depth studies for the growth behavior and the  
10  
11 morphology of  $\langle 111 \rangle$  oriented NWs strongly suggest the NWs have been grown through the self-  
12  
13 catalytic VLS process. Furthermore, the NWs with different growth directions exhibit distinct  
14  
15 morphological features, allowing control of the NW morphology from uniform NWs to 2D-like  
16  
17 NRs structures.  
18  
19

20  
21  
22 Self-catalytic GeNWs grown at low temperature ( $T_g < 320 \text{ }^\circ\text{C}$ ) with the high partial pressure  
23  
24 of Ge precursor ( $\text{GeH}_4$ ) have random growth directions (Fig. S1 in supporting information).  
25  
26 However, under low  $\text{GeH}_4$  partial pressure, NWs predominantly grow in a specific  
27  
28 crystallographic direction, and the direction can be controlled according to the growth temperature  
29  
30 even on the same substrate (Fig. 1). The scanning electron microscope (SEM) image in Figure 1a  
31  
32 shows uniform GeNWs grown at  $340 \text{ }^\circ\text{C}$ . When viewed along the  $[100]$  direction of the substrate  
33  
34 plane, the GeNWs are inclined at  $45 \text{ }^\circ$  and are consistent with the  $\langle 110 \rangle$  growth direction. At  
35  
36  $360 \text{ }^\circ\text{C}$ , most NWs are grown along the  $\langle 112 \rangle$  direction with a slightly tapered morphology (Fig.  
37  
38 1b). The GeNWs grown at temperatures above  $380 \text{ }^\circ\text{C}$  are aligned at a  $90^\circ$  angle normal to the  
39  
40 substrate with the four fixed  $\langle 111 \rangle$  directions, indicating the NWs are  $\langle 111 \rangle$  oriented (Fig. 1c).  
41  
42  
43 Figures 1d-f show high-resolution transmission electron microscope (HRTEM) images and  
44  
45 selected area electron diffraction (SAED) patterns near the tips of the  $\langle 110 \rangle$ ,  $\langle 112 \rangle$ , and  $\langle 111 \rangle$   
46  
47 oriented single-crystalline GeNWs, respectively. The temperature dependence of the NW growth  
48  
49 direction was further verified by the change in the NW growth direction according to the  
50  
51 temperature change during growth (Fig. 2b and Fig. S2). Initially,  $\langle 112 \rangle$ -oriented GeNWs having  
52  
53  
54  
55  
56  
57  
58  
59  
60

1  
2  
3 a rectangular cross-section were grown at 360 °C. When increasing the temperature up to 420 °C  
4  
5  
6 during the growth, the growth direction changes from  $\langle 112 \rangle$  to  $\langle 111 \rangle$ , and the cross-sectional  
7  
8 shape was also changed from rectangular to hexagonal shape.

9  
10 Based on the results, a possible mechanism for the orientation-controlled NW growth is  
11 suggested (Fig. 2a). When supersaturation in the gas phase reaches a critical level, Ge nanocrystal  
12 seeds can be nucleated on the reactive oxide surface.<sup>29</sup> At low growth temperature, the subsequent  
13 formation of stable side facets promotes the anisotropic growth in the  $\langle 110 \rangle$  or  $\langle 112 \rangle$  direction  
14 as precursor species are continuously supplied to the Ge nanowire tip with a high sticking  
15 coefficient. In general, spontaneous growth of crystalline NWs usually progresses in a direction  
16 that shows minimal surface energy at the NW growth tip. Among the low-index facets of Si and  
17 Ge with diamond cubic structure, the  $\{111\}$  and  $\{100\}$  facets have the lowest and second-lowest  
18 surface energy, respectively,<sup>30</sup> and thus  $\langle 112 \rangle$  or  $\langle 110 \rangle$  growth directions with  $\{111\}$  and  $\{100\}$   
19 side facets are energetically favored for the group IV semiconductor NWs grown without an  
20 external catalyst.<sup>27-28, 31</sup> The related thermodynamic studies have been systematically conducted in  
21 the Si and Ge NWs.<sup>32-33</sup> As the temperature increases to 380 °C, the NW tips are presumed to exist  
22 as a fully liquid state due to size-dependent melting point depression. Bulk Ge crystal has a high  
23 melting temperature (937 °C). However, an in-situ TEM study recently demonstrated that Ge  
24 nanoparticles with a diameter of approximately 20 nm readily melt even at temperatures below  
25 400 °C.<sup>34-35</sup> Because the liquid-solid interface at the growth tip prefers  $\{111\}$  solid facets with the  
26 lowest interface energy,<sup>36</sup> GeNWs can grow in the  $\langle 111 \rangle$  growth directions perpendicular to the  
27  $\{111\}$  surfaces, although the surface energy of NW sidewall is higher than that of NWs grown in  
28  $\langle 110 \rangle$  and  $\langle 112 \rangle$  directions (Fig. S3). For Si and Ge NWs, the  $\langle 111 \rangle$  growth direction is a unique  
29 feature observed only in VLS and VLS-like growth to the best of our knowledge.<sup>5, 32, 37</sup>  
30  
31  
32  
33  
34  
35  
36  
37  
38  
39  
40  
41  
42  
43  
44  
45  
46  
47  
48  
49  
50  
51  
52  
53  
54  
55  
56  
57  
58  
59  
60

1  
2  
3 Furthermore, the  $\langle 111 \rangle$ -oriented GeNWs with connected chain-like morphology were  
4  
5 occasionally observed at the high growth temperature (Fig. S4). The lamellar twinning periodically  
6  
7 occurs in the narrow neck of the spherical chains,<sup>38-41</sup> which is due to 2D ledge nucleation and  
8  
9 epitaxial propagation occurring along the liquid-solid  $\{111\}$  interface.<sup>42-43</sup> Similar phenomena are  
10  
11 also observed in crystal growth of undercooled Ge melt, favoring closed-packed  $\{111\}$  facets at  
12  
13 the liquid-solid interface.<sup>44-45</sup> In general, compound solids, such as II-VI or III-V semiconductors,  
14  
15 can grow anisotropically to 1D NWs through the VLS process even without an external catalyst  
16  
17 because one of the elements can act as a liquid catalyst during the NW growth. However, VLS-  
18  
19 based 1D growth of single-element materials has been limitedly studied only in materials, such as  
20  
21 Si and Ge, for which suitable external metal catalysts are available.  
22  
23  
24

25  
26 To investigate the orientation-dependent structural features, GeNWs with  $\langle 110 \rangle$ ,  $\langle 112 \rangle$ , and  
27  
28  $\langle 111 \rangle$  crystal directions were synthesized under  $\text{GeH}_4$  partial pressure of 1.5 Torr with the flow  
29  
30 rate of 40 sccm at  $380^\circ\text{C}$  (Fig. 3a). Although grown under the same conditions, the NWs exhibited  
31  
32 characteristic morphological features depending on the crystal growth direction (Fig. 3b). While  
33  
34 the  $\langle 111 \rangle$ -oriented GeNWs are highly tapered with a relatively low growth rate, the  $\langle 110 \rangle$ -  
35  
36 oriented GeNWs had a much faster growth rate and uniform diameter. The  $\langle 112 \rangle$ -oriented GeNW  
37  
38 showed a moderate growth rate and tapering. Furthermore, it is worth mentioning that the axial  
39  
40 and radial growth rates of GeNWs were strongly dependent on their crystallographic growth  
41  
42 directions, which have rarely been studied before. These interesting phenomena can be explained  
43  
44 by the geometric and thermodynamic properties of the semiconductor NWs enclosed by the crystal  
45  
46 facets with different surface energies. The  $\{112\}$  side plane enclosing  $\langle 111 \rangle$ -oriented GeNW with  
47  
48 hexagonal cross-section has relatively higher surface energy compared with the other low-index  
49  
50 planes.<sup>46</sup> Therefore, Ge adatoms from the vapor precursor species are easily incorporated at the  
51  
52  
53  
54  
55  
56  
57  
58  
60

1  
2  
3 side planes, promoting the radial growth in the  $\langle 111 \rangle$  oriented GeNWs (Fig. 3c). On the other  
4  
5  
6 hand,  $\langle 110 \rangle$  oriented GeNWs have the lowest-energy state owing to the presence of three  $\{111\}$   
7  
8 and three  $\{100\}$  stable planes.<sup>31</sup> Direct precursor impingement for radial growth is suppressed, and  
9  
10 Ge adatoms easily diffuse up to the NW tip. As a result, the growth rate in the axial direction is  
11  
12 much faster even under the same growth conditions, resulting in a uniform shape of  $\langle 110 \rangle$  oriented  
13  
14  
15 GeNWs (Fig. 3e). The  $\langle 112 \rangle$  oriented GeNW has a rectangular cross-section which consists of  
16  
17 two  $\{111\}$  and two  $\{110\}$  side planes.<sup>47</sup> The slightly tapered morphology is related to the  
18  
19 thermodynamic lateral growth on a specific side surface (Fig. 3d).

20  
21  
22 The highly tapered GeNWs growing along the  $[111]$  direction have sawtooth faceting along  
23  
24 the entire NW length (Fig. 4a and Fig. S5). The periodicity of upward and downward  $\{111\}$  facets  
25  
26 is observed, accompanying high-index planes such as  $(115)$ ,  $(557)$ , and  $(119)$  on the side surface  
27  
28  
29 of each  $\{112\}$  of the  $[111]$  oriented GeNW (Figs. 4c-e). This periodic faceting has often been  
30  
31 observed in semiconductor NWs grown *via* metal-catalyzed VLS growth, and it has been attributed  
32  
33 to liquid-solid instability, enhanced vapor-solid (VS) deposition, impurity diffusion, or other  
34  
35  
36 chemical species supplied from the gas phase.<sup>46, 48-50</sup> However, the downward faceting observed  
37  
38 at the base of  $\langle 111 \rangle$  oriented GeNWs indicates that the periodic faceting results from the  
39  
40 competition between interfacial instability and surface energy minimization at the high  
41  
42  
43 temperature (Fig. S6). The surface energy of  $\{112\}$  side planes increases with the elongation of  
44  
45 the NWs, leading to the periodic formation of the  $(111)/(002)$  plane to stabilize the radial growth  
46  
47 perpendicular to the liquid-solid interface of the  $\langle 111 \rangle$  oriented GeNWs. In addition, continuous  
48  
49 VS deposition at a high temperature can induce surface reconstruction on a side plane, resulting in  
50  
51  
52 the formation of the high-index planes.<sup>51-52</sup> In contrast to the highly tapered  $\langle 111 \rangle$  oriented  
53  
54 GeNW,  $\langle 110 \rangle$  oriented GeNW has very uniform morphology along the axial direction because  
55  
56  
57  
58  
59  
60



1  
2  
3 the  $\langle 110 \rangle$  oriented NWs are bounded by a large number of  $\{111\}$  and  $\{110\}$  planes having the  
4  
5 lowest surface energy (Figs. 4f-h).<sup>53-54</sup> Therefore, unintentional Ge deposition on  $\langle 110 \rangle$  oriented  
6  
7 GeNWs could be minimized, thus preventing the formation of tapered morphology of non-uniform  
8  
9 dopant distribution along the NW length.<sup>55-56</sup> Theoretical and experimental studies have also  
10  
11 reported that stable  $\langle 110 \rangle$  NWs can have significantly increased carrier mobility,<sup>57-58</sup> indicating  
12  
13 that the selective preparation of  $\langle 110 \rangle$  oriented NWs may improve reliability as well as  
14  
15 performance in electronic device applications of semiconducting NWs. Otherwise, the  $\langle 112 \rangle$ -  
16  
17 oriented NW of group-IV materials usually has a rectangular cross-section, and its sides consist of  
18  
19 two low-energy  $\{111\}$  and high-energy  $\{110\}$  surfaces.<sup>47</sup> By taking advantage of the energy  
20  
21 difference between the two different facets, we have grown flexible 2D-like GeNRs (Figs. 4i-k).  
22  
23 Ge species can be preferentially adsorbed on unstable  $\{110\}$  planes, eventually leading to  
24  
25 morphological evolution from  $\langle 112 \rangle$  oriented GeNWs to GeNRs. The large width to thickness  
26  
27 ratio also reveals that the lateral growth on the  $\{110\}$  planes simultaneously occurs and competes  
28  
29 with the axial growth of the  $\langle 112 \rangle$  NWs (Fig. S7). To further investigate the anisotropic lateral  
30  
31 growth of the  $\langle 112 \rangle$  oriented GeNWs, we enhanced lateral growth of the  $\langle 112 \rangle$  NWs to  $\langle 110 \rangle$   
32  
33 directions using a two-step process, which clearly shows that different surface energies promote  
34  
35 the preferential growth on the  $\{110\}$  planes (Fig. S8). 2D semiconductor NRs are promising  
36  
37 building blocks for flexible or stretchable electronics.<sup>59-60</sup> However, bottom-up grown NRs have  
38  
39 seldom been observed in group-IV semiconductor materials.  
40  
41  
42  
43  
44

45  
46 In conclusion, we demonstrated that the crystal orientation of self-catalytic GeNWs could be  
47  
48 selectively controlled by adjusting the growth temperature. At low temperature, the  $\langle 110 \rangle$  oriented  
49  
50 GeNWs mainly grow with a uniform diameter along the NW length, while at high-temperature  
51  
52 growth, the  $\langle 111 \rangle$  oriented GeNWs exhibit a highly tapered morphology. At an intermediate  
53  
54  
55  
56  
57  
58  
60

1  
2  
3 temperature, the <112> oriented GeNWs predominantly grow. We also demonstrated that different  
4  
5  
6 crystal orientations play an essential role in determining the geometrical and morphological  
7  
8 features of NWs. In particular, the controlled evolution from rectangular GeNWs to flexible 2D-  
9  
10 like GeNRs is an excellent example of the morphology-controlled growth of novel nanostructures.  
11  
12 The results of this study may provide an opportunity to utilize the orientation-dependent properties  
13  
14 of semiconductor NW in practical device applications. Furthermore, the self-catalytic growth of  
15  
16 the <111> oriented Ge NWs suggests VLS-based NW growth may be possible for a wide range of  
17  
18 single elementary materials even without an external catalyst.  
19  
20  
21  
22  
23

### 24 **Supporting Information**

25  
26 Detailed experimental procedures and Figures S1– S8. The Supporting Information is available  
27  
28 free of charge at <http://pubs.acs.org>.  
29

### 30 **Corresponding Author**

31  
32 \*E-Mail: [dwhang@skku.edu](mailto:dwhang@skku.edu) (D.W); [skku97@gmail.com](mailto:skku97@gmail.com) (B.-S.K.)  
33  
34  
35

### 36 **Notes**

37  
38 The authors declare no competing financial interest.  
39

### 40 **Acknowledgment**

41  
42 This research was supported by the National Research Foundation (NRF-2021R1A2C2013378) of  
43  
44 the Ministry of Science and ICT of Korea and the Korea Basic Science Institute (KBSI) National  
45  
46 Research Facilities & Equipment Center (NFEC) grant funded by the Korea Ministry of Education  
47  
48  
49  
50  
51 (No. 2019R1A6C1010031). BK acknowledges support from Basic Science Research Program  
52  
53  
54  
55  
56  
57  
58  
59  
60

1  
2  
3 through the National Research Foundation of Korea (NRF) funded by the Ministry of Education  
4  
5 (2013R1A6A3A03063814).  
6  
7  
8  
9  
10  
11  
12  
13  
14  
15  
16  
17  
18  
19  
20  
21  
22  
23  
24  
25  
26  
27  
28  
29  
30  
31  
32  
33  
34  
35  
36  
37  
38  
39  
40  
41  
42  
43  
44  
45  
46  
47  
48  
49  
50  
51  
52  
53  
54  
55  
56  
57  
58  
59  
60

## References

1. Cui, Y.; Lieber, C. M., Functional nanoscale electronic devices assembled using silicon nanowire building blocks. *Science* **2001**, *291*, 851-853.
2. Jin, S.; Whang, D.; McAlpine, M. C.; Friedman, R. S.; Wu, Y.; Lieber, C. M., Scalable interconnection and integration of nanowire devices without registration. *Nano Lett.* **2004**, *4*, 915-919.
3. Yan, R.; Gargas, D.; Yang, P., Nanowire photonics. *Nat. Photonics* **2009**, *3*, 569-576.
4. Cui, Y.; Wei, Q.; Park, H.; Lieber, C. M., Nanowire nanosensors for highly sensitive and selective detection of biological and chemical species. *Science* **2001**, *293*, 1289-1292.
5. O'Regan, C.; Biswas, S.; Petkov, N.; Holmes, J. D., Recent advances in the growth of germanium nanowires: Synthesis, growth dynamics and morphology control. *J. Mater. Chem. C* **2014**, *2*, 14-33.
6. Lauhon, L. J.; Gudlksen, M. S.; Wang, D.; Lieber, C. M., Epitaxial core-shell and core-multishell nanowire heterostructures. *Nature* **2002**, *420*, 57-61.
7. Yang, J. E.; Jin, C. B.; Kim, C. J.; Jo, M. H., Band-gap modulation in single-crystalline Si<sub>1-x</sub>Ge<sub>x</sub> nanowires. *Nano Lett.* **2006**, *6*, 2679-2684.
8. Gudiksen, M. S.; Lauhon, L. J.; Wang, J.; Smith, D. C.; Lieber, C. M., Growth of nanowire superlattice structures for nanoscale photonics and electronics. *Nature* **2002**, *415*, 617-620.
9. Nguyen, B. M.; Taur, Y.; Picraux, S. T.; Dayeh, S. A., Diameter-independent hole mobility in Ge/Si Core/shell nanowire field effect transistors. *Nano Lett.* **2014**, *14*, 585-591.
10. Park Ii, W.; Zheng, G.; Jiang, X.; Tian, B.; Lieber, C. M., Controlled synthesis of millimeter-long silicon nanowires with uniform electronic properties. *Nano Lett.* **2008**, *8*, 3004-3009.
11. Filonov, A. B.; Petrov, G. V.; Novikov, V. A.; Borisenko, V. E., Orientation effect in electronic properties of silicon wires. *Appl. Phys. Lett.* **1995**, *67*, 1090.
12. Persson, M. P.; Lherbier, A.; Niquet, Y. M.; Triozon, F.; Roche, S., Orientational dependence of charge transport in disordered silicon nanowires. *Nano Lett.* **2008**, *8*, 4146-4150.
13. Arantes, J. T.; Fazzio, A., Theoretical investigations of Ge nanowires grown along the [110] and [111] directions. *Nanotechnology* **2007**, *18*, 295706.
14. Yang, X. B.; Zhang, R. Q., Indirect-to-direct band gap transitions in phosphorus adsorbed <112> silicon nanowires. *Appl. Phys. Lett.* **2008**, *93*, 173108

- 1  
2  
3 15. Dellas, N. S.; Liu, B. Z.; Eichfeld, S. M.; Eichfeld, C. M.; Mayer, T. S.; Mohny, S. E.,  
4 Orientation dependence of nickel silicide formation in contacts to silicon nanowires. *J. Appl.*  
5 *Phys.* **2009**, *105*, 094309.  
6  
7  
8 16. Yang, H.; Huang, S.; Huang, X.; Fan, F.; Liang, W.; Liu, X. H.; Chen, L. Q.; Huang, J. Y.;  
9 Li, J.; Zhu, T.; Zhang, S., Orientation-dependent interfacial mobility governs the anisotropic  
10 swelling in lithiated silicon nanowires. *Nano Lett.* **2012**, *12*, 1953-1958.  
11  
12  
13  
14 17. Zhao, Q.; Xie, T.; Peng, L.; Lin, Y.; Wang, P.; Peng, L.; Wang, D., Size- and orientation-  
15 dependent photovoltaic properties of ZnO nanorods. *J. Phys. Chem. C* **2007**, *111*, 17136-  
16 17145.  
17  
18  
19 18. Li, X.; Wei, X.; Xu, T.; Pan, D.; Zhao, J.; Chen, Q., Remarkable and crystal-structure-  
20 dependent piezoelectric and piezoresistive effects of InAs nanowires. *Adv. Mater.* **2015**, *27*,  
21 2852-2858.  
22  
23  
24 19. Adhikari, H.; Marshall, A. F.; Chidsey, C. E. D.; McIntyre, P. C., Germanium nanowire  
25 epitaxy: Shape and orientation control. *Nano Lett.* **2006**, *6*, 318-323.  
26  
27 20. Lugstein, A.; Steinmair, M.; Hyun, Y. J.; Hauer, G.; Pongratz, P.; Bertagnolli, E., Pressure-  
28 induced orientation control of the growth of epitaxial silicon nanowires. *Nano Lett.* **2008**, *8*,  
29 2310-2314.  
30  
31  
32 21. Shimizu, T.; Xie, T.; Nishikawa, J.; Shingubara, S.; Senz, S.; Gösele, U., Synthesis of vertical  
33 high-density epitaxial Si(100) nanowire arrays on a Si(100) substrate using an anodic  
34 aluminum oxide template. *Adv. Mater.* **2007**, *19*, 917-920.  
35  
36  
37 22. Wang, J.; Plissard, S. R.; Verheijen, M. A.; Feiner, L. F.; Cavalli, A.; Bakkers, E. P. A. M.,  
38 Reversible switching of InP nanowire growth direction by catalyst engineering. *Nano Lett.*  
39 **2013**, *13*, 3802-3806.  
40  
41  
42 23. Zhang, M. L.; Peng, K. Q.; Fan, X.; Jie, J. S.; Zhang, R. Q.; Lee, S. T.; Wong, N. B.,  
43 Preparation of large-area uniform silicon nanowires arrays through metal-assisted chemical  
44 etching. *J. Phys. Chem. C* **2008**, *112*, 4444-4450.  
45  
46  
47 24. Tsvion, D.; Schwartzman, M.; Popovitz-Biro, R.; Von Huth, P.; Joselevich, E., Guided  
48 growth of millimeter-long horizontal nanowires with controlled orientations. *Science* **2011**,  
49 *333*, 1003-1007.  
50  
51  
52  
53  
54  
55  
56  
57  
58  
59  
60

- 1
  - 2
  - 3
  - 4
  - 5
  - 6
  - 7
  - 8
  - 9
  - 10
  - 11
  - 12
  - 13
  - 14
  - 15
  - 16
  - 17
  - 18
  - 19
  - 20
  - 21
  - 22
  - 23
  - 24
  - 25
  - 26
  - 27
  - 28
  - 29
  - 30
  - 31
  - 32
  - 33
  - 34
  - 35
  - 36
  - 37
  - 38
  - 39
  - 40
  - 41
  - 42
  - 43
  - 44
  - 45
  - 46
  - 47
  - 48
  - 49
  - 50
  - 51
  - 52
  - 53
  - 54
  - 55
  - 56
  - 57
  - 58
  - 59
  - 60
25. Huang, Y. H., Competition between surface energy and interphase energy in transition region and diameter-dependent orientation of silicon nanowires. *Appl. Surf. Sci.* **2009**, *255*, 4347-4350.
26. Schmidt, V.; Senz, S.; Gösele, U., Diameter-dependent growth direction of epitaxial silicon nanowires. *Nano Lett.* **2005**, *5*, 931-935.
27. Tan, T. Y.; Lee, S. T.; Gösele, U., A model for growth directional features in silicon nanowires. *Appl. Phys. A* **2002**, *74*, 423-432.
28. Zhang, R. Q.; Lifshitz, Y.; Lee, S. T., Oxide-assisted growth of semiconducting nanowires. *Adv. Mater.* **2003**, *15*, 635-640.
29. Kim, B. S.; Koo, T. W.; Lee, J. H.; Kim, D. S.; Jung, Y. C.; Hwang, S. W.; Choi, B. L.; Lee, E. K.; Kim, J. M.; Whang, D., Catalyst-free growth of single-crystal silicon and germanium nanowires. *Nano Lett.* **2009**, *9*, 864-869.
30. Stekolnikov, A. A.; Furthmüller, J.; Bechstedt, F., Absolute surface energies of group-IV semiconductors: Dependence on orientation and reconstruction. *Phys. Rev. B* **2002**, *65*, 115318.
31. Hanrath, T.; Korgel, B. A., Crystallography and surface faceting of germanium nanowires. *Small* **2005**, *1*, 717-721.
32. Garcia-Gil, A.; Biswas, S.; Holmes, J. D., A Review of Self-Seeded Germanium Nanowires: Synthesis, Growth Mechanisms and Potential Applications. *Nanomaterials* **2021**, *11*, 2002.
33. Migas, D. B.; Borisenko, V. E.; Rusli; Soci, C., Revising morphology of <111>-oriented silicon and germanium nanowires. *Nano Converg.* **2015**, *2*, 16.
34. Hession, F. X.; Thurmond, C. D.; Trumbore, F. A., On the melting point of germanium. *J. Phys. Chem. C* **1955**, *59*, 1076-1078.
35. Lotty, O.; Hobbs, R.; O'Regan, C.; Hlina, J.; Marschner, C.; O'Dwyer, C.; Petkov, N.; Holmes, J. D., Self-seeded growth of germanium nanowires: Coalescence and ostwald ripening. *Chem. Mater.* **2013**, *25*, 215-222.
36. Wang, H.; Zepeda-Ruiz, L. A.; Gilmer, G. H.; Upmanyu, M., Atomistics of vapour-liquid-solid nanowire growth. *Nat. Commun.* **2013**, *4*, 1956.
37. Schmidt, V.; Wittemann, J. V.; Senz, S.; Gösele, U., Silicon Nanowires: A Review on Aspects of their Growth and their Electrical Properties. *Adv. Mater.* **2009**, *21*, 2681-2702.

- 1  
2  
3 38. Fujiwara, K., Crystal growth behaviors of silicon during melt growth processes. *Int. J.*  
4 *Photoenergy* **2012**, *2012*, 169829.
- 5  
6  
7 39. Hao, Y.; Meng, G.; Wang, Z. L.; Ye, C.; Zhang, L., Periodically twinned nanowires and  
8 polytypic nanobelts of ZnS: The role of mass diffusion in vapor-liquid-solid growth. *Nano*  
9 *Lett.* **2006**, *6*, 1650-1655.
- 10  
11  
12 40. Kutsukake, K.; Abe, T.; Usami, N.; Fujiwara, K.; Morishita, K.; Nakajima, K., Formation  
13 mechanism of twin boundaries during crystal growth of silicon. *Scr. Mater.* **2011**, *65*, 556-  
14 559.
- 15  
16  
17 41. Xiong, Q.; Wang, J.; Eklund, P. C., Coherent twinning phenomena: Towards twinning  
18 superlattices in III-V semiconducting nanowires. *Nano Lett.* **2006**, *6*, 2736-2742.
- 19  
20  
21 42. Hofmann, S.; Sharma, R.; Wirth, C. T.; Cervantes-Sodi, F.; Ducati, C.; Kasama, T.; Dunin-  
22 Borkowski, R. E.; Drucker, J.; Bennett, P.; Robertson, J., Ledge-flow-controlled catalyst  
23 interface dynamics during Si nanowire growth. *Nat. Mater.* **2008**, *7*, 372-375.
- 24  
25  
26 43. Wen, C. Y.; Reuter, M. C.; Tersoff, J.; Stach, E. A.; Ross, F. M., Structure, growth kinetics,  
27 and ledge flow during vapor-solid-solid growth of copper-catalyzed silicon nanowires. *Nano*  
28 *Lett.* **2010**, *10*, 514-519.
- 29  
30  
31 44. Nagashio, K.; Kuribayashi, K., Growth mechanism of twin-related and twin-free facet Si  
32 dendrites. *Acta Mater.* **2005**, *53*, 3021-3029.
- 33  
34 45. Herlach, D. M.; Simons, D.; Pichon, P.-Y., Crystal growth kinetics in undercooled melts of  
35 pure Ge, Si and Ge-Si alloys. *Philos. Trans. Royal Soc. A* **2018**, *376*, 20170205.
- 36  
37  
38 46. Ross, F. M.; Tersoff, J.; Reuter, M. C., Sawtooth faceting in silicon nanowires. *Phys. Rev.*  
39 *Lett.* **2005**, *95*, 146104.
- 40  
41 47. Li, C. P.; Lee, C. S.; Ma, X. L.; Wang, N.; Zhang, R. Q.; Lee, S. T., Growth direction and  
42 cross-sectional study of silicon nanowires. *Adv. Mater.* **2003**, *15*, 607-609.
- 43  
44  
45 48. Li, F.; Nellist, P. D.; Cockayne, D. J. H., Doping-dependent nanofaceting on silicon nanowire  
46 surfaces. *Appl. Phys. Lett.* **2009**, *94*, 263111.
- 47  
48 49. Schwarz, K. W.; Tersoff, J.; Kodambaka, S.; Chou, Y. C.; Ross, F. M., Geometrical  
49 frustration in nanowire growth. *Phys. Rev. Lett.* **2011**, *107*, 265502.
- 50  
51  
52 50. Xu, T.; Nys, J. P.; Addad, A.; Lebedev, O. I.; Urbietta, A.; Salhi, B.; Berthe, M.; Grandidier,  
53 B.; Stiévenard, D., Faceted sidewalls of silicon nanowires: Au-induced structural  
54 reconstructions and electronic properties. *Phys. Rev. B* **2010**, *81*, 115403.
- 55  
56  
57  
58  
59  
60

- 1  
2  
3 51. Baski, A. A.; Whitman, L. J., Quasiperiodic nanoscale faceting of high-index Si surfaces.  
4  
5 *Phys. Rev. Lett.* **1995**, *74*, 956-959.  
6
- 7 52. Baski, A. A.; Whitman, L. J., A scanning tunneling microscopy study of hydrogen adsorption  
8 on Si(112). *J. Vac. Sci. Technol. A* **1995**, *13*, 1469-1472.  
9
- 10 53. Zhu, Y.; Zhu, Y., Growth property of silicon nanowires under OAG. *Int. J. Mod. Phys. B.*  
11 **2005**, *19*, 683-685.  
12
- 13 54. Goldthorpe, I. A.; Marshall, A. F.; McIntyre, P. C., Inhibiting strain-induced surface  
14 roughening: Dislocation-free Ge/Si and Ge/SiGe core-shell nanowires references. *Nano Lett.*  
15 **2009**, *9*, 3715-3719.  
16
- 17 55. Allen, J. E.; Perea, D. E.; Hemesath, E. R.; Lauhon, L. J., Nonuniform nanowire doping  
18 profiles revealed by quantitative scanning photocurrent microscopy. *Adv. Mater.* **2009**, *21*,  
19 3067-3072.  
20
- 21 56. Perea, D. E.; Hemesath, E. R.; Schwalbach, E. J.; Lensch-Falk, J. L.; Voorhees, P. W.;  
22 Lauhon, L. J., Direct measurement of dopant distribution in an individual vapour-liquid-solid  
23 nanowire. *Nat. Nanotechnol.* **2009**, *4*, 315-319.  
24
- 25 57. Buin, A. K.; Verma, A.; Svizhenko, A.; Anantram, M. P., Significant enhancement of hole  
26 mobility in [110] silicon nanowires compared to electrons and bulk silicon. *Nano Lett.* **2008**,  
27 *8*, 760-765.  
28
- 29 58. Murphy-Armando, F.; Fagas, G.; Greer, J. C., Deformation potentials and electron-phonon  
30 coupling in silicon nanowires. *Nano Lett.* **2010**, *10*, 869-873.  
31
- 32 59. Law, M.; Sirbuly, D. J.; Johnson, J. C.; Goldberger, J.; Saykally, R. J.; Yang, P., Nanoribbon  
33 waveguides for subwavelength photonics integration. *Science* **2004**, *305*, 1269-1273.  
34
- 35 60. Sun, Y.; Choi, W. M.; Jiang, H.; Huang, Y. Y.; Rogers, J. A., Controlled buckling of  
36 semiconductor nanoribbons for stretchable electronics. *Nat. Nanotechnol.* **2006**, *1*, 201-207.  
37  
38  
39  
40  
41  
42  
43  
44  
45  
46  
47  
48  
49  
50  
51  
52  
53  
54  
55  
56  
57  
58  
59  
60



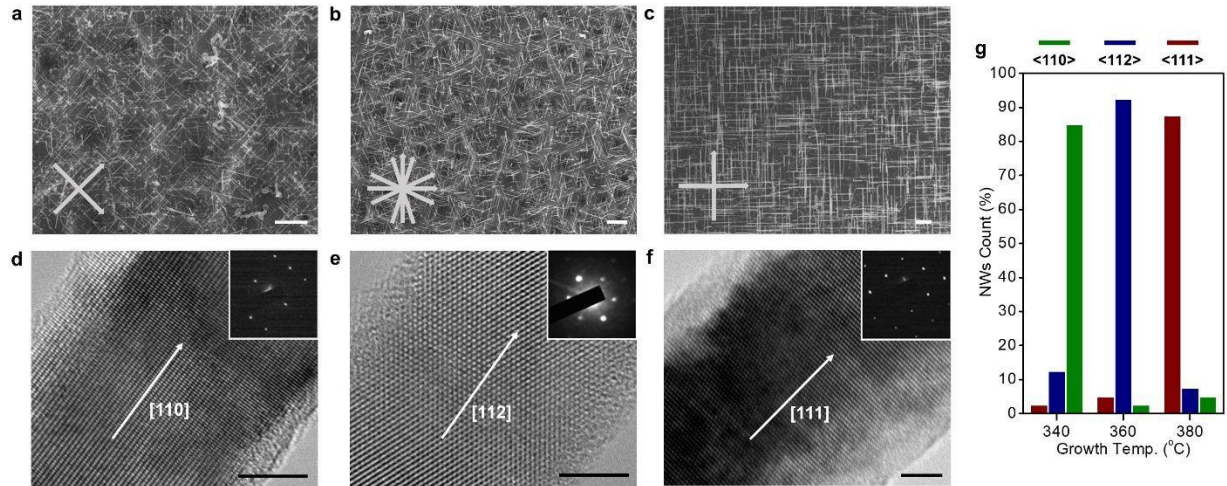


**Figure 1. Temperature-dependent growth of <110>, <112>, and <111> oriented GeNWs.** Plane-view SEM and HRTEM images with the corresponding SAED patterns of self-catalytic GeNWs epitaxially grown on Ge/Si (100) substrates at different temperatures and growth times with other conditions fixed. (a and d) <110> oriented GeNWs at 340 °C. (b and e) <112> oriented GeNWs at 360 °C. (c and f) <111> oriented GeNWs at 380 °C. Inserts show the schematics of the top view images of the <110>, <112>, and <111> directions on the substrate, respectively. Scale bars (a-c), 1  $\mu$ m. Scale bar (inset), 500 nm. Scale bars (d-f), 2 nm. (g) NW counts versus the corresponding growth temperature to control the NW orientation.

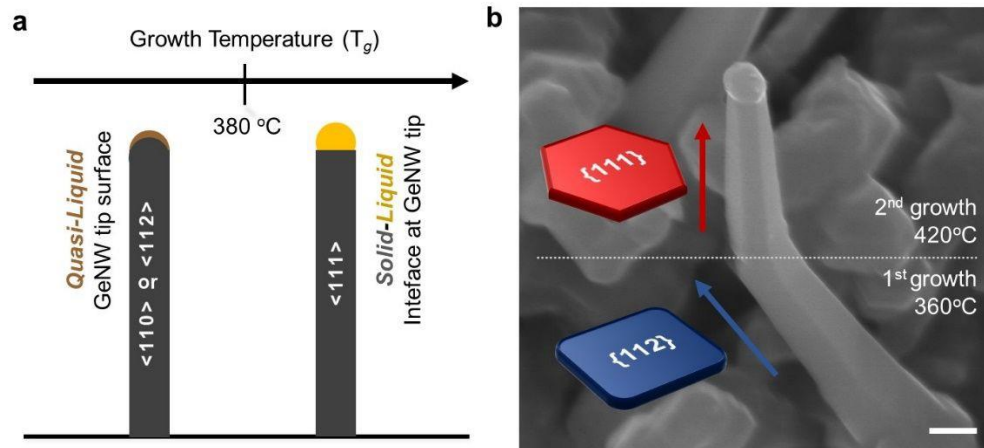


**Figure 2. A suggested mechanism for orientation control and growth direction switching of GeNWs.** (a) Schematic illustration of the self-catalytic growth of GeNWs with a preferential orientation by adjusting growth temperature. (b) An SEM image of the kinked GeNW grown by a two-step process, clearly showing the morphological transition from rectangular <112> to hexagonal <111> oriented GeNW. Insets show NW morphologies at the corresponding growth temperatures. Scale bar, 200 nm.

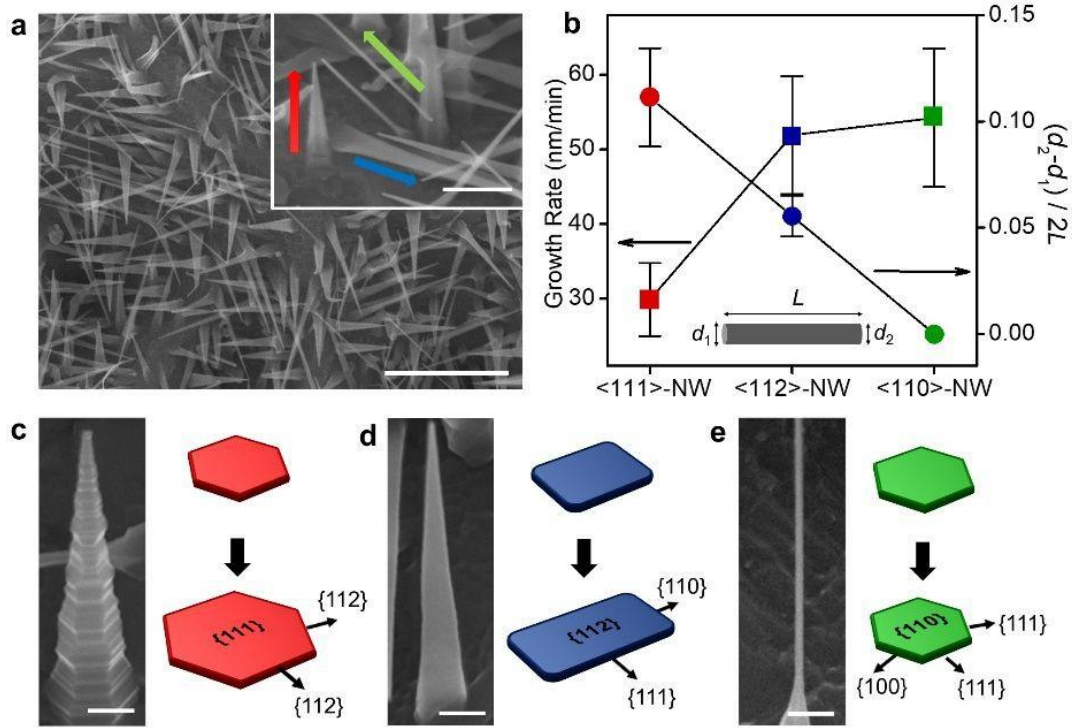


**Figure 3. Orientation-dependent structural properties of GeNWs.** (a) Top-view SEM images of self-catalytic GeNWs grown on Ge/Si(100) substrate at 380 °C with controlled GeH<sub>4</sub> partial pressure of 1.5 Torr. The inset image clearly shows the different NW morphologies and growth rates, dependent on the NW orientations. Scale bars, 200 nm. (b) Tapering degree and growth rate variations of GeNWs with different directions at the same growth condition. (c, d, and e) SEM images and schematic models of the <110>, <112>, and <111> oriented NWs exhibiting the different cross-sections and the orientation-modulated change of NW morphologies. Scale bars, 100 nm.

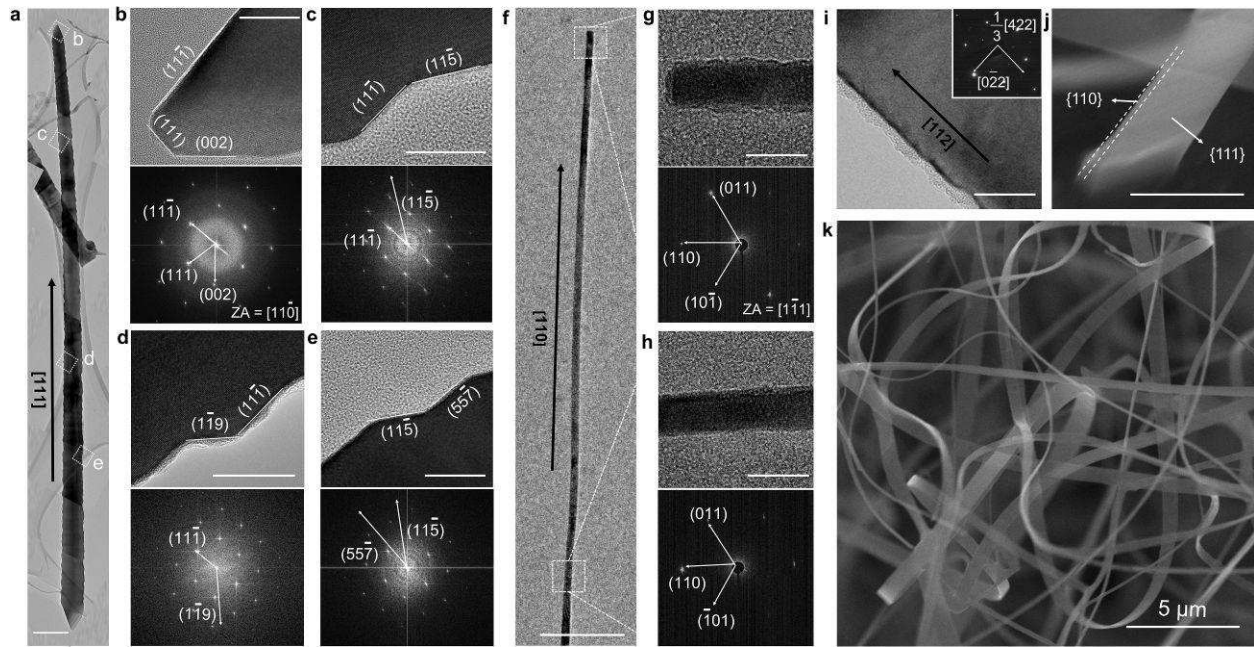


**Figure 4. Crystal structure analysis according to the growth direction of GeNW.** (a) Series of TEM and corresponding FFT images showing single crystal  $[111]$  oriented NW. Scale bar, 200 nm. (b) Tip of GeNW faceted by low-index by low-index  $(11\bar{1})$  and  $(002)$  planes. (c, d, and e) HR images of the sawtooth faceting with a regular periodicity. (f) HR images with the corresponding SAED patterns of  $[110]$  oriented GeNW. (g) NW growth tip and (h) body with an atomically smooth surface. (i and j) SEM and TEM images of the single crystalline GeNRs, confirming that the GeNRs have a rectangular shape with two  $\{111\}$  and two  $\{1\bar{1}0\}$  directions. The inset of (i) is an FFT image corresponding with the same GeNRs. (k) SEM image of GeNRs which evolved from  $\langle 112 \rangle$  oriented GeNWs. Scale bars in (a), (f) and (j), 200 nm. Scale bars in (b-e), (g), (h), and (i), 20 nm.

For Table of Contents Only

